J. Fluid Mech. (1999), *vol.* 388, *pp.* 259–288. Printed in the United Kingdom

Can the atmospheric kinetic energy spectrum be explained by two-dimensional turbulence?

By ERIK LINDBORG

Department of Mechanics, KTH, S-100 44 Stockholm, Sweden
e-mail: erikl@mech.kth.se

(Received 20 March 1998 and in revised form 23 December 1998)

The statistical features of turbulence can be studied either through spectral quantities, such as the kinetic energy spectrum, or through structure functions, which are statistical moments of the difference between velocities at two points separated by a variable distance. In this paper structure function relations for two-dimensional turbulence are derived and compared with calculations based on wind data from 5754 airplane flights, reported in the MOZAIC data set. For the third-order structure function two relations are derived, showing that this function is generally positive in the two-dimensional case, contrary to the three-dimensional case. In the energy inertial range the third-order structure function grows linearly with separation distance and in the enstrophy inertial range it grows cubically with separation distance. A Fourier analysis shows that the linear growth is a reflection of a constant negative spectral energy flux, and the cubic growth is a reflection of a constant positive spectral enstrophy flux. Various relations between second-order structure functions and spectral quantities are also derived. The measured second-order structure functions can be divided into two different types of terms, one of the form $r^{2/3}$, giving a $k^{-5/3}$-range and another, including a logarithmic dependence, giving a k^{-3}-range in the energy spectrum. The structure functions agree better with the two-dimensional isotropic relation for larger separations than for smaller separations. The flatness factor is found to grow very fast for separations of the order of some kilometres. The third-order structure function is accurately measured in the interval [30, 300] km and is found to be positive. The average enstrophy flux is measured as $\Pi_\omega \approx 1.8 \times 10^{-13}\,\mathrm{s}^{-3}$ and the constant in the k^{-3}-law is measured as $\mathscr{K} \approx 0.19$. It is argued that the k^{-3}-range can be explained by two-dimensional turbulence and can be interpreted as an enstrophy inertial range, while the $k^{-5/3}$-range can probably not be explained by two-dimensional turbulence and should not be interpreted as a two-dimensional energy inertial range.

1. Introduction

The kinetic energy spectrum of atmospheric air motion at high and middle altitudes is a challenge to atmospheric physics as well as theoretical fluid dynamics. In figure 1 the mesoscale and large-scale spectrum is reproduced from Nastrom, Gage & Jasperson (1984). This spectrum was calculated from wind measurements taken from over six thousand commercial air flights during the years 1975 to 1979. The most distinctive feature of the spectrum is of course the extended $k^{-5/3}$-range in the mesoscale region from wavelengths of some few kilometres to wavelengths of approximately

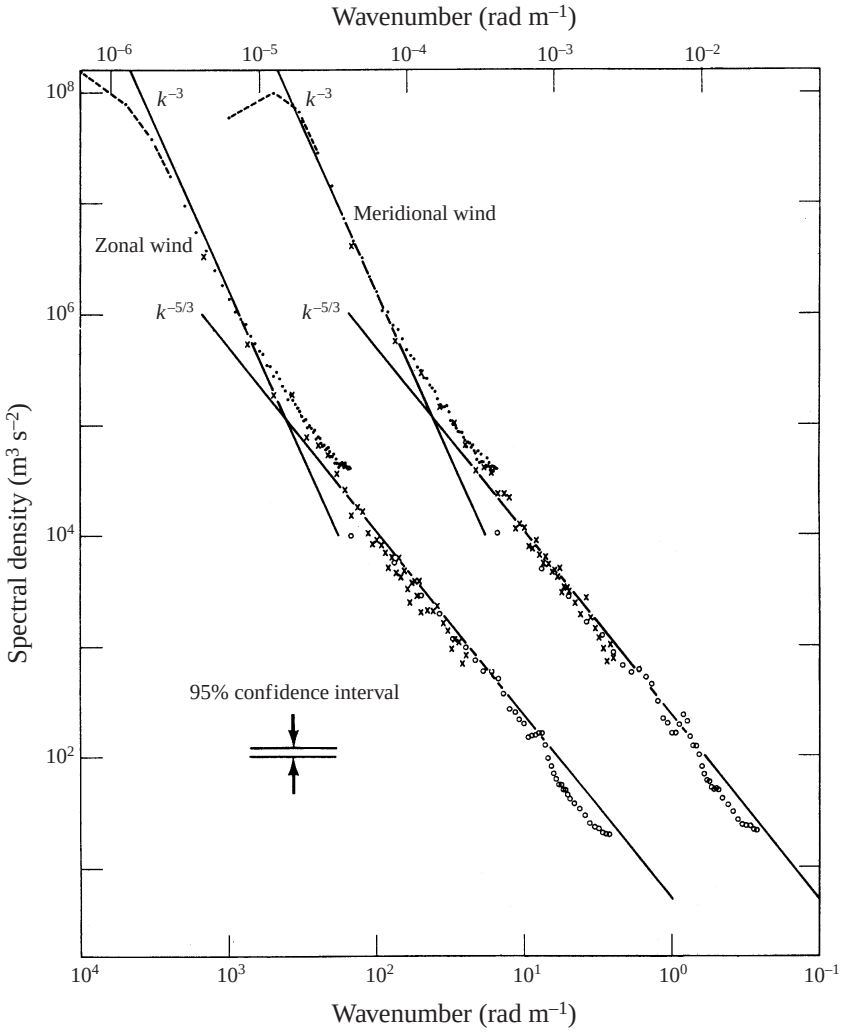

FIGURE 1. Kinetic energy spectrum near the tropopause from GASP aircraft data. The spectrum for meridional winds is shifted one decade to the right. Spectral averages based on long- (•), short- (○) and intermediate- (×) scale data are shown. Reprinted by permission from *Nature* (Nastrom *et al.* 1984), copyright 1984 Macmillan Magazines Ltd.

500 km. Nastrom *et al.* (1984) also identified a rather narrow range of wavelengths of 1000–3000 km with a -3 power law dependence of the energy spectrum.

Two different hypotheses have been put forward to explain the $k^{-5/3}$-range of the spectrum. First, is (Dewan 1979; VanZandt 1982) that the $k^{-5/3}$-range can be explained by internal gravity waves. According to this hypothesis long gravity waves break down to shorter waves in a continuous chain, resulting in a positive energy flux from large to small scales, very much in the same way as three-dimensional Kolmogorov turbulence. The only parameter which can determine the spectrum is the energy flux and from dimensional considerations we obtain the $k^{-5/3}$-spectrum. Secondly, there is the hypothesis (Gage 1979) that the $k^{-5/3}$-spectrum is the spectrum of two-dimensional turbulence with a negative energy flux, i.e. a flux from small to large scales, in accordance with Kraichnan's (1967, 1970) theory of two-dimensional turbulence. Such

a range naturally emerges in two-dimensional direct numerical simulations (DNS) with forcing at large wavenumbers (Smith & Yakhot 1994; Maltrud & Vallis 1991).

The k^{-3}-range is usually interpreted as a two-dimensional enstrophy inertial range in the sense of Kraichnan's theory. In such a range, enstrophy (half the square of vorticity) is nonlinearly transferred from large to small scales. The only parameter which can determine the energy spectrum is the flux of enstrophy. This single parameter dependence leads to the k^{-3}-spectrum. Such a spectrum has very rarely been observed in DNS and recently the enstrophy inertial range interpretation of the atmospheric spectrum has been seriously questioned (Smith & Yakhot 1994).

Thus, there are two questions of fundamental importance in this field which are yet to be answered: Is the $k^{-5/3}$-range a two-dimensional energy inertial range and is the k^{-3}-range a two-dimensional enstrophy inertial range? There are various possible combinations of answers to these two questions, even for scientists adhering to the two-dimensional turbulence hypothesis. To get a better grasp of the different possibilities we first repeat the elementa of the theory of two-dimensional turbulence as developed by Kraichnan (1967, 1970).

Kraichnan considered turbulence created by a random force concentrated around a fairly large wavenumber in Fourier space, as compared to the smallest wavenumbers which are determined by the size of the physical system which is studied. The force is injecting energy as well as enstrophy into the system. He demonstrated that in the absence of vortex stretching the nonlinear inertial force will have the effect of transferring energy from large to small wavenumbers, i.e. from small to large scales. This is in the opposite direction as compared to three-dimensional turbulence. If the Reynolds number is large there should be a region where inertial forces are dominating and where the only parameter determining the energy spectrum, $E(k)$, of the flow is the rate, Π_u, at which energy is propagating through the spectrum. By dimensional considerations we must then have

$$E(k) = C_0 \mid \Pi_u \mid^{2/3} k^{-5/3}, \tag{1}$$

in this range. C_0 is here a dimensionless constant. We have taken the absolute value of Π_u since Π_u by definition is taken to be negative when the flux is in the direction towards small wavenumbers.

In the absence of vortex stretching the nonlinear term in the two-dimensional Navier–Stokes equations will conserve enstrophy as well as energy. Kraichnan showed that at the same time as energy is propagating to smaller wavenumbers from the source concentrated at a specific wavenumber, enstrophy will propagate in the opposite direction from the same source. If the Reynolds number is sufficiently large there should be a range of fairly high wavenumbers where inertial forces are dominating and where the only parameter determining the statistics of the flow is the rate, Π_ω, at which enstrophy is propagating through the spectrum. By dimensional considerations we obtain

$$E(k) = \mathscr{K} \Pi_\omega^{2/3} k^{-3}, \tag{2}$$

in this range. $\mathscr{K}$ is a dimensionless constant. Kraichnan also suggested that (2) should include a correcting logarithmic factor.

It is of course tempting to apply this theory directly to the atmospheric spectrum, shown in figure 1, and identify the $k^{-5/3}$-range with a two-dimensional energy inertial range with an inverse energy cascade and identify the k^{-3}-range with a two-dimensional enstrophy inertial range with a forward enstrophy cascade. However, several objections can be raised against such a straightforward interpretation.

First of all, the two-dimensional turbulence hypothesis seems to require an energy source which has its maximum at scales of the order of one kilometre, where a transition zone between micro- and meso-scale spectra is visible (Vinnichenko 1970). It can be argued that three-dimensional effects should be dominating at such small scales. Fluctuations at these scales should therefore lead to a downward three-dimensional energy flux to smaller scales and not an upward energy flux to larger scales. However, there is some evidence that a two-dimensional inverse energy cascade can emerge even when the forcing is applied in scales which are small enough to be truly three-dimensional. In DNS of quasi-two-dimensional box turbulence in a rotating frame of reference Smith, Chasnov & Waleffe (1996) found that three-dimensional forcing at small scales (comparable with the height of the box) led to an inverse two-dimensional energy cascade. Whether this is the case in the atmosphere is a question which ultimately must be answered by measurements.

Another objection to the two-dimensional turbulence interpretation of the atmospheric spectrum is that the k^{-3}-range appears for smaller wavenumbers than the $k^{-5/3}$-range, contrary to the predictions of Kraichnan. Since the work of Kraichnan it has become something of a scientific paradigm that the enstrophy inertial range with the k^{-3}-spectrum — if it exists at all — must appear for larger wavenumbers than those where we find the $k^{-5/3}$-spectrum. For example, Frisch (1995) finds it 'paradoxical' that the $k^{-5/3}$-range in the atmosphere is found for larger wavenumbers than the k^{-3} range.

Gage & Nastrom (1986) suggested that there could be an energy and enstrophy sink in the intermediate region of wavelengths from 500 to 1000 km. This sink would dissipate both energy and enstrophy and thus prohibit the range of constant energy flux to overlap with the range of constant enstrophy flux. In a sense, this would save the paradigm of two non-overlapping ranges. However, as noted by Gage & Nastrom, the change from $k^{-5/3}$ to k^{-3} in the region of 500 km is very smooth, and it is difficult to believe that a dissipative force concentrated at this scale would not be more clearly reflected in the energy spectrum. It is also difficult to imagine what sort of physical force there could be which could provide this powerful sink at scales of about 500 km.

Another possibility would be that the $k^{-5/3}$-range of the atmosphere can be interpreted as a two-dimensional energy inertial range in the sense of Kraichnan's theory, while the k^{-3}-range cannot be interpreted as an enstrophy inertial range. After all the k^{-3}-range is rather narrow, and there might be some other reason why the spectrum has this shape. Smith & Yakhot (1994) have suggested that the k^{-3}-spectrum is not a sign of an enstrophy inertial range, but can be expained as a 'pile up' of energy caused by the finite size of the Earth together with the so-called 'β-effect' (differential rotation). The k^{-3}-range has very seldom been observed in direct numerical simulations. In most simulations the slope of the spectrum is steeper in the range of constant enstrophy flux. In recent years a great many scientists have questioned that the k^{-3}-range can be a universal feature even for high Reynolds number two-dimensional turbulence. It is often argued that the presence of long-lived coherent structures should make the energy spectrum steeper.

In spite of all these objections there is still a consistent way to interpret both the $k^{-5/3}$-range and the k^{-3}-range in the light of the two-dimensional turbulence theory, without any introduction of an intermediate energy sink. It is noticeable that Kraichnan only considered the case with one force term acting at fairly small scales. With such a single force the enstrophy inertial range must appear for larger wavenumbers than the energy inertial range, with the wavenumber corresponding to the force in between. He did not consider the case with one large-scale force and

one small-scale force. Lilly (1989) suggested that this is the case which is relevant to the atmosphere. He argued that it is quite possible that a combined energy and enstrophy inertial range can appear in the intermediate region between a large-scale force, originating from baroclinic instability at wavelengths of several thousands of kilometres, and a small-scale force due to convective and shearing instabilities at small wavelengths. In such a range enstrophy from the large-scale force would propagate to smaller scales at the same time as energy from the small-scale force would propagate in the opposite direction. That such a range can exist has been shown by Maltrud & Vallis (1991) in a DNS of two-dimensional turbulence on a β-plane. Introducing two separated force terms they found a distinct intermediate region with an overlapping negative energy flux and a positive enstrophy flux. A rather narrow $k^{-5/3}$-range was also observed while the energy spectrum was considerably steeper than k^{-3} for smaller wavenumbers. In the present article we shall also show analytically, that such a combined energy and enstrophy inertial range can emerge in the case where there is both a large-scale and a small-scale source of energy.

Discussing different hypotheses within the two-dimensional turbulence school, we should not forget that the fundamental question is yet to be answered. Can the atmospheric spectrum be interpreted at all as the spectrum of quasi-two-dimensional turbulence? In trying to answer this question we have chosen to measure structure functions rather than spectral quantities. We have made this choice for several reasons.

The energy spectrum in the upper troposphere and lower stratosphere has previously been investigated in a number of studies, for example by Vinnichenko (1970), Kao & Wendell (1970), Balsley & Carter (1982), Nastrom *et al.* (1984) and Nastrom & Gage (1985). It is not very likely that another study of the energy spectrum would add much information to the existing knowledge. It is true that structure functions also have been measured in the atmosphere, for example by Van Atta & Chen (1970) and Antonia, Zhu & Hosokawa (1995). However, these measurements were made at lower altitudes and for smaller scales to investigate three-dimensional turbulence. To our knowledge, no structure function analysis has previously been made to investigate large-scale horizontal dynamics of the atmosphere.

Structure functions can be evaluated in a more straightforward way than corresponding spectral quantities. In a spectral analysis the data series have to be divided into sections with a certain length and the mean velocity has to removed. This procedure involves a certain degree of arbitrariness, and can also lead to errors, both in the low-wavenumber part and the high-wavenumber part of a spectrum computed on a section with a certain length. This arbitrariness is avoided when structure functions are calculated. In this case there is no need to divide the data series into sections and remove the mean velocity. Another advantage is that in a structure function investigation there is a direct connection between the concept of 'scale' and the result of the actual measurement. The calculated structure function for a certain separation distance will correspond directly to measurements of the velocity at two points separated by the same distance. This is of course not true for a spectral analysis. The connection between wavenumber and length scale is not at all as direct. The advantage of a spectral formulation, on the other hand, is that the energy and enstrophy contents within a certain wavenumber interval can be directly computed from the spectrum. The structure functions in a certain separation distance interval do not, in the same way, tell us anything about the energy or enstrophy contents within this interval. Thus, the two formulations can give us complementary pictures of the same phenomenon.

The main reason, however, for calculating structure functions, rather than spectral quantities, is the possibility of determining the energy and enstrophy fluxes by measur-

ing third-order structure functions. This is a possibility which has not been recognized previously. In this paper, we shall derive the relations between the third-order structure functions and the spectral flux of energy and enstrophy. In principle, the fluxes could also be measured in spectral space, by calculating the energy and enstrophy transfer functions, but such an analysis would require knowledge of the entire two-dimensional velocity field. Airplane measurements offer only one-dimensional data sequences.

Another test of the two-dimensional turbulence theory is to investigate whether longitudinal and transverse structure functions agree with the two-dimensional isotropic relation. In particular, this is a test of the two-dimensionality of the small-scale part of the spectrum, i.e. the $k^{-5/3}$-range. If two-dimensionality prevails down to scales of the order of some few kilometres, we must expect a very close agreement with isotropic relations at these scales, especially when the structure functions are calculated from a large number of data recordings from airplanes flying in different directions at different latitudes over the Earth.

In the first part of this article we shall derive the structure function relations by which the two-dimensional interpretation of the atmospheric energy spectrum can be empirically tested. In the second part we shall present structure functions calculated from commercial aircraft wind data reported in the MOZAIC data set.

2. Kolmogorov's law

The third-order structure function law (Kolmogorov 1941*b*) for three-dimensional turbulence

$$\langle \delta u_L \delta u_L \delta u_L \rangle = -\tfrac{4}{5}\epsilon r \tag{3}$$

is a cornerstone in turbulence theory. Here $\delta \boldsymbol{u} = \boldsymbol{u}' - \boldsymbol{u}$, is the difference between the velocity at two points $\boldsymbol{x}'$ and $\boldsymbol{x}$, L indicates the component in the direction of the separation vector $\boldsymbol{r} = \boldsymbol{x}' - \boldsymbol{x}$, ϵ is the average dissipation range and $\langle\ \rangle$ means the ensemble average. This law has been verified by several measurements, for example in the boundary layer of the atmosphere by Van Atta & Chen (1970) and by Antonia *et al.* (1995) and in a marine boundary layer by Van Atta & Park (1980) as well as in the NASA Ames wind tunnel by Saddoughi & Veravalli (1994). It can be shown (Frisch 1995; Lindborg 1996) that the law (3) is a reflection of the existence of a constant positive energy flux in the inertial range of Fourier space. It is a special case of a more general energy flux relation (Lindborg 1996; Antonia *et al.* 1997)

$$\langle \delta u_L \delta u_L \delta u_L \rangle + 2\langle \delta u_L \delta u_T \delta u_T \rangle = -\tfrac{4}{3}\epsilon r, \tag{4}$$

where T indicates a transverse direction, i.e. a direction perpendicular to $\boldsymbol{r}$.

There are two important properties of (4) which are of particular relevance for the present investigation. First, we note that the minus sign on the right-hand side of (4) means that the spectral energy flux Π_u is positive, i.e. in the direction from small to large wavenumbers. A positive right-hand side would have meant that the energy flux was in the opposite direction. Secondly, the relation offers us a method of measuring the dissipation and thereby the magnitude of the energy flux by making a measurement in much larger scales than those in which dissipation occurs, and at the same time in much smaller scales than those in to which energy is fed.

In two-dimensional turbulence there are two possible inertial ranges: an energy inertial range with a constant negative spectral energy flux and an enstrophy inertial range with a positive spectral enstrophy flux. Here we shall derive two counterparts of Kolmogorov's law for two-dimensional turbulence, one for the energy inertial range

and one for the enstrophy inertial range, and show how they relate to the spectral flux of energy and enstrophy. We shall also demonstrate that a combined energy and enstrophy inertial range will most likely appear in the case when there is a large-scale enstrophy source and a small-scale energy source.

3. Derivation for two-dimensional turbulence

The incompressible Navier–Stokes equations can be written

$$\frac{\partial \boldsymbol{u}}{\partial t} + \boldsymbol{u} \cdot \nabla \boldsymbol{u} = -\frac{1}{\rho}\nabla p + \nu \nabla^2 \boldsymbol{u} + \boldsymbol{f}, \tag{5}$$

where $\boldsymbol{f}$ is a force term which we do not specify. In a rotating frame of reference there is also a Coriolis force term on the right-hand side, but this term is not relevant in the present analysis, since we shall study the energy equation in which the Coriolis force does not appear. From the Navier–Stokes equations we can derive the equation for the two-point correlation function, $\langle \boldsymbol{u} \cdot \boldsymbol{u}' \rangle$, of homogeneous incompressible turbulence. This equation can be written

$$\frac{\partial}{\partial t}\langle \boldsymbol{u} \cdot \boldsymbol{u}' \rangle = \tfrac{1}{2}\nabla \cdot \langle \delta \boldsymbol{u}\, \delta \boldsymbol{u} \cdot \delta \boldsymbol{u} \rangle + 2\nu \nabla^2 \langle \boldsymbol{u} \cdot \boldsymbol{u}' \rangle + \langle \boldsymbol{u} \cdot \boldsymbol{f}' \rangle + \langle \boldsymbol{u}' \cdot \boldsymbol{f} \rangle, \tag{6}$$

where the derivatives here are taken with respect to the separation vector $\boldsymbol{r}$. The equation is derived by multiplying the $\boldsymbol{u}$-equation by $\boldsymbol{u}'$ and the $\boldsymbol{u}'$-equation by $\boldsymbol{u}$, adding the two resulting equations, taking the ensemble average and using the condition of homogeneity (see Frisch 1995). For homogeneous turbulence we have the relation (see Batchelor 1953)

$$\nabla^2 \langle \boldsymbol{u} \cdot \boldsymbol{u}' \rangle = -\langle \boldsymbol{\omega} \cdot \boldsymbol{\omega}' \rangle, \tag{7}$$

where $\boldsymbol{\omega}$ is the vorticity vector. In plane two-dimensional turbulence $\boldsymbol{\omega}$ has only one non-zero component, pointing up from the plane. Denoting this component by ω and applying the Laplace operator on (6) we find

$$-\frac{\partial}{\partial t}\langle \omega \omega' \rangle = \tfrac{1}{2}\nabla^2 \left(\nabla \cdot \langle \delta \boldsymbol{u}\, \delta \boldsymbol{u} \cdot \delta \boldsymbol{u} \rangle \right) + 2\nu \nabla^4 \langle \boldsymbol{u} \cdot \boldsymbol{u}' \rangle + \nabla^2 \langle \boldsymbol{u} \cdot \boldsymbol{f}' \rangle + \nabla^2 \langle \boldsymbol{u}' \cdot \boldsymbol{f} \rangle. \tag{8}$$

In two-dimensional turbulence the single-point limit of the triple correlation term in (8) is zero, due to the fact that there is no vortex stretching in two dimensions. This is the important property of two-dimensional turbulence which we shall make use of in this derivation.

The enstrophy equation is obtained as half the single-point limit of (8)

$$\frac{\partial \Omega}{\partial t} = -\epsilon_\omega + Q, \tag{9}$$

where $\Omega = \langle \omega \omega \rangle / 2$ is the enstrophy,

$$\epsilon_w = \nu \langle \nabla \omega \cdot \nabla \omega \rangle \tag{10}$$

is the rate of enstrophy dissipation and

$$Q = -\nabla^2 \langle \boldsymbol{u} \cdot \boldsymbol{f}' \rangle \,|_{r=0} \tag{11}$$

is the enstrophy input power. By using the enstrophy equation (9) the two-point

equation (8) can be rewritten as

$$2\epsilon_\omega - 2Q + \frac{\partial}{\partial t}\frac{\langle \delta\omega\delta\omega\rangle}{2} = \tfrac{1}{2}\nabla^2\left(\nabla\cdot\langle \delta\boldsymbol{u}\,\delta\boldsymbol{u}\cdot\delta\boldsymbol{u}\rangle\right) + \nu\nabla^2\langle\delta\omega\delta\omega\rangle + \nabla^2\langle\boldsymbol{u}\cdot\boldsymbol{f}'\rangle + \nabla^2\langle\boldsymbol{u}'\cdot\boldsymbol{f}\rangle. \tag{12}$$

Now we introduce the assumption of local isotropy (Kolmogorov 1941*a*). We do this in two steps. First, we use the assumption only for scalar quantities. That a scalar function $F = F(r,\theta)$ is isotropic means that it is independent of direction, i.e. $F = F(r)$. If F is an averaged quantity and the averaging has been performed over all possible directions then F must be independent of angle. In this case the assumption can be interpreted merely as a consequence of the averaging procedure. Restricting the assumption of isotropy to scalar quantities gives us the opportunity to use it on a truly anisotropic field, provided that we form our field quantities as averages over all direction. We also note that Coriolis terms and pressure terms cannot break the isotropy of the scalar quantities, since these terms do not appear in the scalar equation. We also assume that the time-derivative of the vorticity structure function in (12) is negligible. Using these assumptions, multiplying the equation by 2 and inverting the Laplace operator we find

$$\nabla\cdot\langle\delta\boldsymbol{u}\,\delta\boldsymbol{u}\cdot\delta\boldsymbol{u}\rangle = (\epsilon_\omega - Q)r^2 + 4P - 2\langle\boldsymbol{u}\cdot\boldsymbol{f}'\rangle - 2\langle\boldsymbol{u}'\cdot\boldsymbol{f}\rangle - 2\nu\langle\delta\omega\delta\omega\rangle, \tag{13}$$

where

$$P = \langle\boldsymbol{u}\cdot\boldsymbol{f}\rangle \tag{14}$$

is the energy input power due to the driving force.

For the quasi-two-dimensional case we have to make a somewhat refined analysis in which we take the double limit $r/L \to 0, r/\eta \to \infty$, where L is the very largest length scale and η is the Kolmogorov scale of the three-dimensional cascade. In the atmosphere, L is of the order the radius of the Earth and η is the order of a centimetre. In this double limit, we can expect to find a three-dimensional Kolmogorov energy cascade, for which we have the relation (see Frisch 1995, or Lindborg 1996)

$$\nabla\cdot\langle\delta\boldsymbol{u}\,\delta\boldsymbol{u}\cdot\delta\boldsymbol{u}\rangle = -4\epsilon. \tag{15}$$

Since the derivative of a constant is zero, the triple correlation term in (8) is still zero in the limit under consideration and the enstrophy equation (9) will still be valid, if Ω is interpreted as large-scale enstrophy due to large-scale vertical vorticity. The only difference from the previous analysis will be that a term 4ϵ will appear when we invert the Laplace operator, by virtue of (15). Therefore, P should be replaced by $P - \epsilon$ in (13). This has a very simple explanation. Some of the injected energy will be lost to smaller scales in a three-dimensional energy cascade and finally dissipated at a rate ϵ.

Now we will study the balance in equation (13) for two different cases. The first is when there is only a small-scale force term. This is the case which was studied by Kraichnan (1967, 1970). The second case is when there is a large-scale force term in addition to the small-scale force term. This case has been studied in a direct numerical simulation by Maltrud & Vallis (1991). We will see that there is a qualitative difference between these two cases.

3.1. *Small-scale force*

When there is only a small-scale force and no large-scale force we can distinguish three possible ranges, corresponding to successively increasing separation distance r:

Dissipation range

In the three-dimensional case we have $\langle(\delta u)^3\rangle \sim r^3$ in the range of the very smallest separations, while we have $\langle(\delta u)^3\rangle \sim r^5$ in the two-dimensional case. We show this for the simplest case of local homogeneity and isotropy by taking the mean value of the ensemble average $\langle(\delta u_L)^3\rangle$, formed in two perpendicular directions x and y with corresponding velocity components u and v. For small separations we find

$$\langle(\delta u_L)^3\rangle = \frac{1}{2}\left(\left\langle\left(\frac{\partial u}{\partial x}\right)^3\right\rangle + \left\langle\left(\frac{\partial v}{\partial y}\right)^3\right\rangle\right) r^3 + \frac{1}{4}\left(\frac{\partial}{\partial x}\left\langle\left(\frac{\partial u}{\partial x}\right)^3\right\rangle + \frac{\partial}{\partial y}\left\langle\left(\frac{\partial v}{\partial y}\right)^3\right\rangle\right) r^4 + O(r^5). \tag{16}$$

The first term vanishes due to incompressibility, since $\partial v/\partial y = -\partial u/\partial x$ in two dimensions. The second term vanishes due to homogeneity, while the term of $O(r^5)$ does not generally vanish. Since $\langle(\delta u)^3\rangle \sim r^5$ in the immediate neighbourhood of the origin, the main balance in (13) is within the terms on the right-hand side, which can be seen from the expansions:

$$2\nu\langle\delta\omega\delta\omega\rangle = \epsilon_\omega r^2 + O(r^4), \tag{17}$$

$$2\langle\boldsymbol{u}\cdot\boldsymbol{f}'\rangle + 2\langle\boldsymbol{u}'\cdot\boldsymbol{f}\rangle = 4P - Qr^2 + O(r^4). \tag{18}$$

Enstrophy inertial range

In this range r is sufficiently large for the inequality

$$2\nu\langle\delta\omega\delta\omega\rangle \ll \epsilon_\omega r^2 \tag{19}$$

to hold, but still sufficiently small for the equality

$$2\langle\boldsymbol{u}\cdot\boldsymbol{f}'\rangle + 2\langle\boldsymbol{u}'\cdot\boldsymbol{f}\rangle = 4P - Qr^2 \tag{20}$$

to hold with good approximation. Thus, a condition for the existence of such a range is that the correlation length between the velocity and the force is not too small, i.e. the turbulence is not significantly forced in its very smallest scales. If we integrate (13) over a disc with radius r in the enstrophy inertial range we find

$$\int_0^{2\pi} \boldsymbol{n}\cdot\langle\delta\boldsymbol{u}\,\delta\boldsymbol{u}\cdot\delta\boldsymbol{u}\rangle\,\mathrm{d}\theta = \frac{\pi}{2}\epsilon_\omega r^3, \tag{21}$$

where $\boldsymbol{n} = \boldsymbol{r}/r$ is the outward pointing normal unit vector of the disc. Here, it has been assumed that the viscous term can be neglected. By the local isotropy hypothesis the integrand is independent of angle and we find

$$\boldsymbol{n}\cdot\langle\delta\boldsymbol{u}\,\delta\boldsymbol{u}\cdot\delta\boldsymbol{u}\rangle = \langle\delta u_L\delta u_L\delta u_L\rangle + \langle\delta u_L\delta u_T\delta u_T\rangle = \tfrac{1}{4}\epsilon_\omega r^3\,. \tag{22}$$

Since we are now working in two dimensions there is only one transverse component and not two as in the three-dimensional relation (4).

Now we assume that not only are scalar quantities isotropic but also the whole third-order structure function tensor, which of course is a much stronger assumption. It is possible to show that the two components in (22) are related through

$$\langle\delta u_L\delta u_T\delta u_T\rangle = \frac{r}{3}\frac{\mathrm{d}}{\mathrm{d}r}\langle\delta u_L\delta u_L\delta u_L\rangle \tag{23}$$

in this case. We derive this relation in the Appendix. Consequently, we obtain

$$\langle \delta u_L \delta u_L \delta u_L \rangle = \langle \delta u_L \delta u_T \delta u_T \rangle = \tfrac{1}{8} \epsilon_\omega r^3. \tag{24}$$

Energy inertial range

In this range r is sufficiently large not only for the inequality (19) to hold but also for the inequality

$$| \, 2\langle \boldsymbol{u} \cdot \boldsymbol{f}' \rangle + 2\langle \boldsymbol{u}' \cdot \boldsymbol{f} \rangle \, | \ll 4P \tag{25}$$

to hold. At the same time we assume that

$$| \, (\epsilon_\omega - Q) r^2 \, | \ll 4P. \tag{26}$$

By integrating (13) over a disc with radius r in the energy inertial range we find

$$\int_0^{2\pi} \boldsymbol{n} \cdot \langle \delta \boldsymbol{u} \, \delta \boldsymbol{u} \cdot \delta \boldsymbol{u} \rangle \, \mathrm{d}\theta = 4\pi P r, \tag{27}$$

where again the viscous term has been neglected. By the local isotropy hypothesis the integrand is independent of angle and we obtain

$$\langle \delta u_L \delta u_L \delta u_L \rangle + \langle \delta u_L \delta u_T \delta u_T \rangle = 2Pr. \tag{28}$$

Again using the stronger assumption that the whole tensor is isotropic we obtain

$$\langle \delta u_L \delta u_L \delta u_L \rangle = \tfrac{3}{2} Pr, \tag{29}$$

$$\langle \delta u_L \delta u_T \delta u_T \rangle = \tfrac{1}{2} Pr. \tag{30}$$

The positive sign on the right-hand side of (28) is a reflection of the fact that the energy flux is in the direction from small to large r, whereas the minus sign in the three-dimensional third-order structure function law (4) is a reflection of the fact that the energy flux in this case is in the opposite direction.

The important feature of the case with a small-scale energy source, studied by Kraichnan (1967), is that the enstrophy inertial range appears for smaller separations (and larger wavenumbers) than the energy inertial range. We shall now contrast this classical case with the case when there is both a small-scale force and a large-scale force.

3.2. *Small-scale and large-scale force*

We now assume that the force term in the Navier–Stokes equations can be divided into two terms

$$\boldsymbol{f} = \boldsymbol{f}_\mathrm{L} + \boldsymbol{f}_\mathrm{S}, \tag{31}$$

where $\boldsymbol{f}_\mathrm{L}$ is a force acting at large-scales and $\boldsymbol{f}_\mathrm{S}$ is a force acting at small scales. When (31) is substituted into (13) one of the terms that will appear on the right-hand side is $-2\langle \boldsymbol{u} \cdot \boldsymbol{f}'_\mathrm{L} \rangle - 2\langle \boldsymbol{u}' \cdot \boldsymbol{f}_\mathrm{L} \rangle$. Since $\boldsymbol{f}_\mathrm{L}$ is a large-scale force this term can be expanded for small values of r. Expanding to second-order we obtain

$$\nabla \cdot \langle \delta \boldsymbol{u} \, \delta \boldsymbol{u} \cdot \delta \boldsymbol{u} \rangle = 4P_\mathrm{S} + Q_\mathrm{L} r^2 - 2\langle \boldsymbol{u} \cdot \boldsymbol{f}'_\mathrm{S} \rangle - 2\langle \boldsymbol{u}' \cdot \boldsymbol{f}_\mathrm{S} \rangle - 2\nu \langle \delta\omega \delta\omega \rangle, \tag{32}$$

where P_S is the energy input power due to the small-scale force and Q_L is the enstrophy input power due to the large-scale force. In the quasi-two-dimensional case with a three-dimensional Kolmogorov range in the limit of small separations P_S should be replaced by $P_\mathrm{S} - \epsilon$. To derive (32) we have assumed that the total enstrophy input

power is equal to the enstrophy dissipation, i.e. $Q_L + Q_S = \epsilon_\omega$. Assuming that r is sufficiently large for the last three terms to be neglected and integrating we find

$$\int_0^{2\pi} \boldsymbol{n} \cdot \langle \delta \boldsymbol{u}\, \delta \boldsymbol{u} \cdot \delta \boldsymbol{u} \rangle \, \mathrm{d}\theta = 4\pi P_S r + \frac{\pi}{2} Q_L r^3, \tag{33}$$

and

$$\langle \delta u_L \delta u_L \delta u_L \rangle + \langle \delta u_L \delta u_T \delta u_T \rangle = 2P_S r + \tfrac{1}{4} Q_L r^3. \tag{34}$$

This relation shows that it is possible and even likely that a combined energy and enstrophy inertial range will appear in the intermediate region between a small-scale and a large-scale force. From equation (34) we see that the influence from the enstrophy source term will be felt more strongly for larger separations while the influence from the energy source term will be felt more strongly for smaller separations in such a combined energy and enstrophy inertial range.

4. Fourier analysis

We shall now make a Fourier analysis of the combined energy and enstrophy inertial range relation (33) and show that this relation means that there is a constant enstrophy flux in the direction from small to large wavenumbers at the same time as there is a constant energy flux in the opposite direction. The Fourier analysis can of course also be carried out separately for the two cases of a pure enstrophy inertial range and a pure energy inertial range.

First we introduce the Fourier transform of the two-point correlation function

$$\widehat{\langle \boldsymbol{u} \cdot \boldsymbol{u}' \rangle} = \frac{1}{(2\pi)^2} \int \langle \boldsymbol{u} \cdot \boldsymbol{u}' \rangle \exp(-\mathrm{i}\boldsymbol{k} \cdot \boldsymbol{r}) \, \mathrm{d}^2 r, \tag{35}$$

with the inverse transform

$$\langle \boldsymbol{u} \cdot \boldsymbol{u}' \rangle = \int \widehat{\langle \boldsymbol{u} \cdot \boldsymbol{u}' \rangle} \exp(\mathrm{i}\boldsymbol{k} \cdot \boldsymbol{r}) \, \mathrm{d}^2 k. \tag{36}$$

The Fourier transform of the third-order structure function is defined in the corresponding way. The two-dimensional energy spectrum is defined by

$$E(k) = \pi k \widehat{\langle \boldsymbol{u} \cdot \boldsymbol{u}' \rangle}, \tag{37}$$

and the energy transfer function is defined by

$$T(k) = \frac{\pi k \mathrm{i}\boldsymbol{k} \cdot \widehat{\langle \delta \boldsymbol{u}\, \delta \boldsymbol{u} \cdot \delta \boldsymbol{u} \rangle}}{2}. \tag{38}$$

In Fourier space equation (6) takes the well-known form

$$\frac{\partial E(k)}{\partial t} = T(k) - 2\nu k^2 E(k) + F(k) \tag{39}$$

where $F(k)$ is the spectrum corresponding to the force term in (6). The spectral flux of energy through wavenumber k is defined by

$$\Pi_u(k) = -\int_0^k T(q) \mathrm{d}q, \tag{40}$$

and the spectral flux of enstrophy is defined by

$$\Pi_\omega(k) = -\int_0^k q^2 T(q)\mathrm{d}q. \tag{41}$$

Now we express $\langle \delta\boldsymbol{u}\,\delta\boldsymbol{u}\cdot\delta\boldsymbol{u}\rangle$ as a Fourier integral and substitute the expression into (33):

$$\int_0^{2\pi}\int \boldsymbol{n}\cdot\widehat{\langle \delta\boldsymbol{u}\,\delta\boldsymbol{u}\cdot\delta\boldsymbol{u}\rangle}\exp(\mathrm{i}\boldsymbol{k}\cdot\boldsymbol{r})\,\mathrm{d}^2k\,\mathrm{d}\theta = 4\pi P_\mathrm{S}\,r + \frac{\pi}{2}Q_\mathrm{L}\,r^3. \tag{42}$$

Integrating in the variable θ we find

$$\int \frac{J_1(kr)}{k}\mathrm{i}\boldsymbol{k}\cdot\widehat{\langle \delta\boldsymbol{u}\,\delta\boldsymbol{u}\cdot\delta\boldsymbol{u}\rangle}\,\mathrm{d}^2k = 2P_\mathrm{S}\,r + \tfrac{1}{4}Q_\mathrm{L}\,r^3, \tag{43}$$

where J_1 is the first-order cylindrical Bessel function.

In a range where both the viscous term and the force term in (39) can be neglected the transfer function $T(k)$ will be approximately equal to zero. The contribution to the integral (43) from the inertial range will therefore be negligible, as will the contribution from higher wavenumbers due to the fast oscillations of the Bessel function for high wavenumbers. Thus, if k_i is a wavenumber in the inertial range the contribution to the integral will come from wavenumbers which are much smaller than k_i. For such wavenumbers $kr \ll 1$ and the Bessel function can be expanded as

$$J_1(kr) = \frac{kr}{2} - \frac{(kr)^3}{16} + O((kr)^5). \tag{44}$$

Thus we find to the second-order

$$\frac{\mathrm{i}\,r}{2}\int_{k<k_\mathrm{i}} \boldsymbol{k}\cdot\widehat{\langle \delta\boldsymbol{u}\,\delta\boldsymbol{u}\cdot\delta\boldsymbol{u}\rangle}\,\mathrm{d}^2k - \frac{\mathrm{i}r^3}{16}\int_{k<k_\mathrm{i}} k^2\boldsymbol{k}\cdot\widehat{\langle \delta\boldsymbol{u}\,\delta\boldsymbol{u}\cdot\delta\boldsymbol{u}\rangle}\,\mathrm{d}^2k = 2P_\mathrm{S}\,r + \tfrac{1}{4}Q_\mathrm{L}\,r^3. \tag{45}$$

Equating orders in r and using the definitions of the energy and enstrophy flux we obtain

$$\Pi_u(k_\mathrm{i}) = -P_\mathrm{S}, \tag{46}$$

$$\Pi_\omega(k_\mathrm{i}) = Q_\mathrm{L}. \tag{47}$$

Thus we have found that the third-order structure function law (34) of real space corresponds to a constant negative spectral energy flux and a constant positive enstrophy flux through Fourier space. The negative energy flux is equal to the energy input power due to the small-scale force and the positive enstrophy flux is equal to the enstrophy input power due to the large-scale force. In the quasi-two-dimensional case with a three-dimensional Kolmogorov range in the limit of small separations, P_S should be replaced by $P_\mathrm{S} - \epsilon$. In this case the negative spectral energy flux is equal to the energy input power minus the three-dimensional energy flux towards small scales.

5. Second-order quantities

5.1. *The energy inertial range*

The energy inertial range hypothesis can be formulated either for the velocity structure function (Kolmogorov 1941*a*), or for the one- or two-dimensional energy spectrum. First we establish the correspondence between the structure function formulation and

the one-dimensional spectrum formulation. We assume that there is a broad inertial range where the second-order structure function has the form

$$\langle \delta \boldsymbol{u} \cdot \delta \boldsymbol{u} \rangle = C \mid \Pi_u \mid^{2/3} \mid x \mid^{2/3}, \tag{48}$$

where x is the distance coordinate of the point at which $\boldsymbol{u}'$ is measured relative to the point at which $\boldsymbol{u}$ is measured. The one-dimensional Fourier transform of the two-point correlation function can be written

$$\widehat{\langle \boldsymbol{u} \cdot \boldsymbol{u}' \rangle} = \delta(k_1) \langle \boldsymbol{u} \cdot \boldsymbol{u} \rangle - \frac{1}{2\pi} \int_{-\infty}^{\infty} \tfrac{1}{2} \langle \delta \boldsymbol{u} \cdot \delta \boldsymbol{u} \rangle \exp(-\mathrm{i} k_1 x) \, \mathrm{d}x. \tag{49}$$

For wavenumbers corresponding to distances in the inertial range the Fourier transform can be approximated by assuming that (48) is valid on the whole real axis. Summing the contributions from negative and positive wavenumbers we obtain the one-dimensional energy spectrum

$$E_1(k) = -C \mid \Pi_u \mid^{2/3} \cos\left(\tfrac{5}{6}\pi\right) \Gamma\left(\tfrac{5}{3}\right) k^{-5/3} = 0.12 C \mid \Pi_u \mid^{2/3} k^{-5/3}. \tag{50}$$

Here we have used the theory of generalized Fourier transforms (see Lighthill 1959). This is the standard procedure of demonstrating the correspondence between a structure function power law and an energy spectrum power law. We shall give experimental evidence confirming that this procedure leads to accurate results.

To establish the correspondence between the structure function formulation and the two-dimensional energy spectrum formulation we use the relation

$$\widehat{\nabla^2 f} = -k^2 \hat{f}, \tag{51}$$

where f is any function and the hat has the meaning of the two-dimensional Fourier transform. Applying the Laplace operator to (48) and using (51) we obtain the two-dimensional energy spectrum

$$\begin{aligned} E(k) &= \tfrac{1}{9} C \mid \Pi_u \mid^{2/3} k^{-5/3} \int_0^{\infty} \tau^{-1/3} J_0(\tau) \, \mathrm{d}\tau \\ &= \frac{2^{-1/3} \Gamma\left(\frac{1}{3}\right)}{9 \Gamma\left(\frac{2}{3}\right)} C \mid \Pi_u \mid^{2/3} k^{-5/3} \approx 0.17 C \mid \Pi_u \mid^{2/3} k^{-5/3}. \end{aligned} \tag{52}$$

The two-dimensional isotropic relation between the longitudinal and transverse second-order structure functions is

$$\langle \delta u_T \delta u_T \rangle = \frac{\mathrm{d}}{\mathrm{d}r} \left(r \langle \delta u_L \delta u_L \rangle \right). \tag{53}$$

We derive this relation in the Appendix. We shall use (53) as a test of the two-dimensionality of the atmospheric spectrum at scales of the order of some few kilometres. For this purpose it could be of some interest to compare it with the corresponding three-dimensional axisymmetric relation. If the scales of the order of some kilometres are three-dimensional we must expect them to be symmetric with respect to vertical axes to a very high degree of accuracy. If we denote the projection of $\boldsymbol{r}$ onto the horizontal plane by ρ, the projection onto the vertical axis by z, the radial velocity component by u, the azimuthal component by v and the axial (or vertical) component by w, we can derive the relation (Lindborg 1995)

$$\langle \delta v \delta v \rangle = \frac{\partial}{\partial \rho} \left(\rho \langle \delta u \delta u \rangle \right) + \rho \frac{\partial}{\partial z} \langle \delta u \delta w \rangle. \tag{54}$$

In the two-dimensional limit there is no dependence on the vertical coordinate z, the vertical velocity w is zero and (54) becomes identical to (53). If the calculated structure functions do not agree with (53) for separation distances of the order of some kilometres, we can conclude with high certainty that these scales are not two-dimensional, but rather axisymmetric, since the last term in (54), including both z-dependence and the vertical velocity increment δw, must be non-zero in this case.

It could also be useful to calculate the value we can expect to find for the skewness

$$S = \frac{\langle \delta u_L \delta u_L \delta u_L \rangle}{\langle \delta u_L \delta u_L \rangle^{3/2}} \tag{55}$$

in a two-dimensional inertial range. In the single-point limit, this quantity becomes identical to the skewness of the velocity derivative $\partial u/\partial x$, which is often studied. In most numerical simulations the two-dimensional Kolmogorov constant is found to be $C_0 \approx 6$. Using this value and the relations (29), (52) and (53), we calculate the skewness as $S \approx 0.03$. This is in agreement with the observation by Smith & Yakhot (1994) that the third-order structure function is small in two-dimensional turbulence. In a three-dimensional inertial range S is negative and about ten times larger in magnitude.

5.2. *The enstrophy inertial range*

We first show that the structure function hypothesis which corresponds to the k^{-3}-energy spectrum can be formulated for the vorticity structure function as

$$\langle \delta\omega \delta\omega \rangle = 4\mathscr{K} \Pi_\omega^{2/3} \ln(r/\eta_\omega) + B \Pi_\omega^{2/3} \tag{56}$$

where $\mathscr{K}$ and B are constants and $\eta_\omega = \nu^{1/2}/\Pi_\omega^{1/6}$ is the Kolmogorov enstrophy length scale. Using the theory of generalized Fourier transforms we find that (56) gives the one-dimensional enstrophy spectrum

$$\Phi_1(k) = \mathscr{K} \Pi_\omega^{2/3} k^{-1}, \tag{57}$$

and the corresponding one-dimensional energy spectrum

$$E_1(k) = \tfrac{1}{2} \mathscr{K} \Pi_\omega^{2/3} k^{-3}. \tag{58}$$

To determine the two-dimensional energy spectrum in the enstrophy inertial range we use the relation

$$\nabla^2 \ln(r) = 2\pi \delta(\boldsymbol{r}), \tag{59}$$

which is easily derived by integrating $\nabla^2 \ln(r)$ over a circle with centre at the origin and using the divergence theorem and the fact that $\nabla^2 \ln(r)$ is equal to zero everywhere except at the origin. Relation (59) together with (51) used twice gives us the two-dimensional energy spectrum

$$E(k) = \mathscr{K} \Pi_\omega^{2/3} k^{-3}. \tag{60}$$

This is Kraichnan's scaling hypothesis.

It could be of some interest to note that the logarithmic law (56) can be derived exactly in the same way as the logarithmic law for the mean velocity in a turbulent boundary layer was derived by Millikan (1939). To do this we assume that the vorticity structure function can be written

$$\langle \delta\omega \delta\omega \rangle = \Pi_\omega^{2/3} f\left(\frac{r}{\eta_\omega}\right), \tag{61}$$

for small separations, and

$$\langle \delta\omega \delta\omega \rangle = 4\Omega - \Pi_\omega^{2/3} g\left(\frac{r}{L}\right), \tag{62}$$

for large separations. Here L is a typical length of the large vortices. Matching these expressions we can derive the log-law (56) in the intermediate range where $\eta_\omega \ll r \ll L$. The expression corresponding to Millikan's friction law will be

$$\frac{\Omega}{\Pi_\omega^{2/3}} = \mathscr{K} \ln\left(\frac{L}{\eta_\omega}\right) + D, \tag{63}$$

where D is a constant, supposedly of the order of unity. A condition for the matching region to occur is that $\ln(L/\eta_\omega)$ must be sufficiently large, probably appreciably larger than unity. This is a condition which is met very slowly when the Reynolds number is increased. The corresponding condition for the occurrence of an energy inertial range in two or three dimensions is that $(L/\eta)^{2/3}$ is larger than unity, where η is the Kolmogorov scale. This condition is met much faster with increasing Reynolds number. The reason why the k^{-3}-spectrum has been so rarely obtained in direct numerical simulations could be that the Reynolds number is far too low in DNS. The ratio L/η_ω is at most of the order of 10^3 in DNS, whereas in the atmosphere it is much larger.

To determine the velocity structure function in the enstrophy inertial range we use the relation

$$\nabla^2 \langle \delta \boldsymbol{u} \cdot \delta \boldsymbol{u} \rangle = -\langle \delta\omega \delta\omega \rangle + 4\Omega. \tag{64}$$

Inserting (56) into (64) and integrating we find

$$\langle \delta \boldsymbol{u} \cdot \delta \boldsymbol{u} \rangle = -\mathscr{K}\, \Pi_\omega^{2/3} r^2 \ln(r/\eta_\omega) + \left[\left(\mathscr{K} - \tfrac{1}{4}B\right) \Pi_\omega^{2/3} + \Omega\right] r^2 + F \ln(r/\eta_\omega) + G, \tag{65}$$

where F and G are integration constants having the dimension of velocity squared. If the enstrophy inertial range is interpreted as an intermediate region between two highly separated length scales η_ω and L and if these are the only physical length scales which are given, then F and G must both be equal to zero, since neither of these two length scales can be relevant in the intermediate region.

5.3. *Overlapping energy and enstrophy inertial ranges*

In the previous section we have shown that if the Reynolds number is sufficiently large, a combined energy and enstrophy inertial range can appear in two-dimensional turbulence. In such a range there is a large- to small-scale constant enstrophy flux and at the same time a small- to large-scale constant energy flux. Another possibility is an enstrophy inertial range overlapping a forward flux energy inertial range, in which three-dimensional effects are important. Which, if any, of these two possibilities is, in fact, the case in the atmosphere must be answered by measurements. In any case an overlap range is controlled by the two parameters Π_u and Π_ω. If we were free to mix these parameters in all possible combinations, together with the separation distance r, then we would not be able to determine the structure function or the energy spectrum using only dimensional considerations. However, it is reasonable to assume that the influence of Π_u on the second-order structure function is felt more strongly for small separation distances and that the influence of Π_ω is felt more strongly for larger separations. Generally, we therefore assume that the two parameters should not be mixed. In accordance with this reasoning we make the assumption that the velocity structure function in a combined energy and enstrophy inertial range is a simple

superposition of the two terms that we have found in previous sections, i.e.

$$\langle \delta \boldsymbol{u} \cdot \delta \boldsymbol{u} \rangle = C \mid \Pi_u \mid^{2/3} r^{2/3} - \mathscr{K} \Pi_\omega^{2/3} r^2 \ln(r/\eta_\omega) + \left[\left(\mathscr{K} - \tfrac{1}{4} B \right) \Pi_\omega^{2/3} + \Omega \right] r^2. \quad (66)$$

The corresponding one-dimensional energy spectrum is

$$E_1(k) = C_1 \mid \Pi_u \mid^{2/3} k^{-5/3} + \tfrac{1}{2} \mathscr{K} \Pi_\omega^{2/3} k^{-3}, \quad (67)$$

where $C_1 \approx 0.12C$. We shall compare the structure function and the energy spectrum calculated from airplane data with these two expressions.

6. From theory to experiment

Provided with the analytical tools by which the two-dimensional turbulence hypothesis can be tested, we now turn to the experimental part of our study. In this part we present the results of structure function calculations based on wind measurements from 5754 commercial flights during the period August 94 to April 97. The airplanes were flying in the upper troposphere and the lower stratosphere, at an altitude of about 10 000 m. The flights are spread all over the globe, with some concentration over northern America, Europe and the northern Atlantic. The total effective data recording time is more than 34 000 hours which is nearly 4 years. The measurements have been made as a part of the MOZAIC program (Measurement of Ozone by Airbus in-service aircraft), which was launched in 1993 by European scientists, aircraft manufacturers and airlines with the aim of performing extended measurements of ozone and water vapour in the atmosphere using commercial long-range airliners. More information about the MOZAIC program can be found in Marenco *et al.* (1998). The wind was recorded from the onboard computor which was linked to the navigation system. It is reported with an accuracy of 0.01 m s^{-1}, but the typical true error is probably larger than this. The accuracy given in the GASP data (Nastrom *et al.* 1984) is 0.5 m s^{-1}. Thanks to Professor Nastrom we have had the opportunity of making a comparative structure function calculation on a set of 89 flights from the GASP data set. For the second-order structure functions the results are, on the whole, similar to those presented here, but for the smallest separations, of the order of a few kilometres, the results from the GASP data set indicate that there is a small but visible round-off error, which is not visible in the results calculated from the MOZAIC data set. We therefore conclude that the typical true error in the MOZAIC data set is no larger than 0.5 m s^{-1}.

There are, of course, different types of variations within all the data which we have used. However, we will treat it as one set, containing samples of essentially the same type of atmospheric process. We will not investigate the variability with respect to altitude, latitude, season or land/sea since an extensive investigation of this type by Nastrom & Gage (1985) found a remarkably small variation of the energy spectrum with respect to all these parameters. We also use Taylor's frozen turbulence hypothesis which means that we calculate structure functions as if the measurements at two points were taken simultaneously. This is motivated if it can be assumed that the time interval, Δt, between the two measurements is much smaller than the typical time scale, T, of variation of atmospheric dynamical processes, i.e. if the speed of the airplane is much higher than the typical relative velocity $|\delta u|$. The speed of the airplane is typically 250 m s^{-1}. From our measured structure functions we can estimate $|\delta u| \sim 4$ m s^{-1} for 100 km and $|\delta u| \sim 30$ m s^{-1} for 1000 km. These estimates indicate that the use of Taylor's hypothesis is not totally unproblematic for separations of the order of 1000 km. Bacmeister *et al.* (1996) have made an extensive

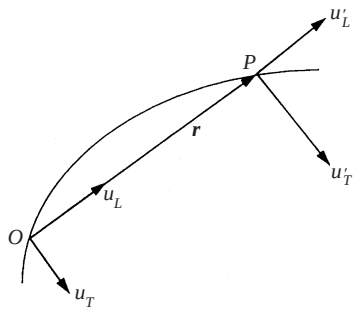

FIGURE 2. The horizontal wind is measured at the points O and P along the flight. $\boldsymbol{r}$ is the separation vector between the points. L indicates the component aligned with $\boldsymbol{r}$ and T a perpendicular component.

analysis of the applicability of Taylor's hypothesis for airplane data analysis, and they conclude that it can be used regardless of the dynamical content in the data. A simple symmetry argument shows that the error introduced by the use of Taylor's hypothesis is quadratic in Δt, rather than linear, when structure functions are calculated. The result of the calculations must be independent of the direction of the time axis, and the error must therefore be even in Δt, which means that the relative error is of the order of $(\Delta t/T)^2$, at most. For scales of the order of 1000 km, $\Delta t \sim 1$ hour, while T is definitely larger. There is no visible deviation from an expected behaviour in our curves for the largest separations, and we therefore trust that Taylor's hypothesis can be used.

7. Results

We have calculated second-, third- and fourth-order structure functions of the longitudinal and transverse velocity increments, $\delta u_L = u'_L - u_L$ and δu_T (see figure 2), in the interval [2, 2510] km; δu_T was chosen in such a way that δu_L and δu_T formed a left-handed system on the northern hemisphere and a right-handed system on the southern hemisphere. But this is of no relevance in the present study where we present results for structure functions which are invariant with respect to right- and left-handedness. The structure functions were calculated with separation distance intervals: 2 km in [2, 50] km, 4 km in [50,150] km, 8 km in [150, 350] km, 16 km in [350, 750], 32 km in [750, 1550] km and 64 km in [1550, 2510] km. Data from 5754 flights were used. Zonal and meridional winds were recorded every fourth second, corresponding to an average interval of one kilometre. The first and last 200 data points of each flight, near start and landing, were not used. Every other point was used as the foot point for all separation distances. The other point was picked as the point coming nearest the specified distance. The structure functions were calculated directly from the recorded wind data, without any removal of the mean velocity, which always must be somewhat arbitrarily defined. No interpolation and no postprocessing was performed on the data. All points presented are the points which are computed in this straightforward way. The results for the second- and the fourth-order structure functions are very well converged over the whole interval. To check this the data were divided into four randomly chosen subsets of about equal size. Calculations based on these subsets gave practically identical results to those presented here. The results for the third-order structure functions are reasonably converged in the interval [30, 300] km.

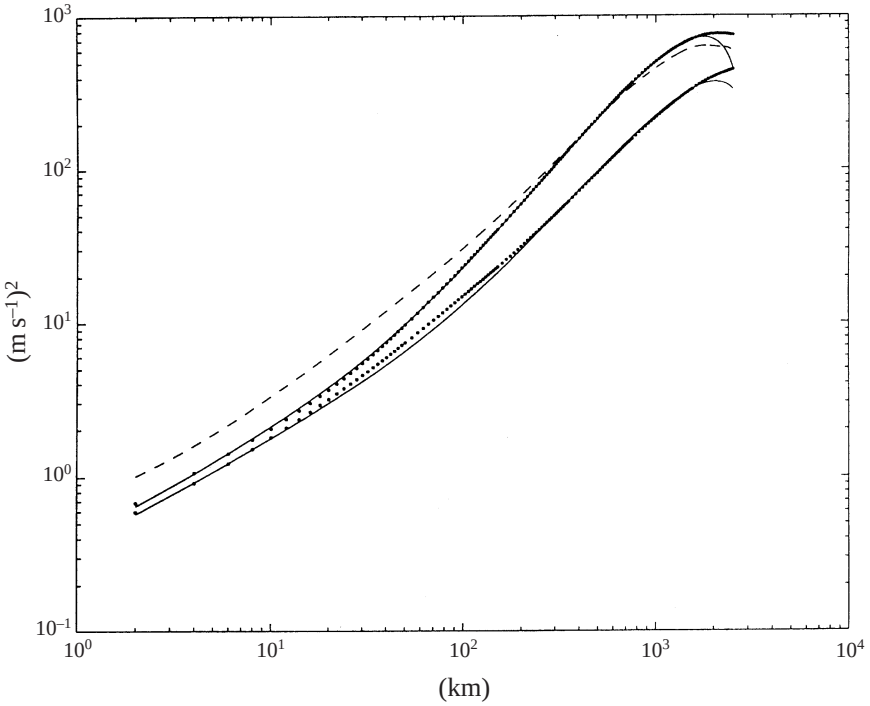

FIGURE 3. Transverse and longitudinal second-order structure functions versus separation distance. The upper curve is the transverse function. Solid lines are curves given by (68) and (69). Dashed line is the isotropic transverse function calculated using the longitudinal function and the relation (53).

7.1. *Second-order structure functions*

In figure 3 we have plotted the second-order longitudinal and transverse structure functions in a log-log plot. The upper curve is the transverse structure function and the lower curve is the longitudinal structure function. The dashed line is the expected isotropic transverse structure function computed according to the two-dimensional relation (53). It was calculated using an eighth-order polonomial fit to the measured longitudinal structure function. The solid lines are best fits to curves given by the relation (66), that is

$$\langle \delta u_L \delta u_L \rangle = a_1 r^{2/3} + b_1 r^2 - c_1 r^2 \ln r, \tag{68}$$

$$\langle \delta u_T \delta u_T \rangle = a_2 r^{2/3} + b_2 r^2 - c_2 r^2 \ln r. \tag{69}$$

The values of the constants were calculated as $a_1 \approx 3.6 \times 10^{-3}$, $a_2 \approx 4.0 \times 10^{-3}$, $b_1 \approx 2.4 \times 10^{-9}$, $b_2 \approx 6.5 \times 10^{-9}$, $c_1 \approx 0.16 \times 10^{-9}$ and $c_2 \approx 0.43 \times 10^{-9}$, where all lengths and times are measured in metres and seconds.

First of all we note that the range with a clearly visible $r^{2/3}$-dependence is rather narrow as compared to the corresponding $k^{-5/3}$-range in the energy spectrum given by Nastrom *et al.* (1984) (see figure 1). The $r^{2/3}$-range is visible only up to separations of about 10 km, while the $k^{-5/3}$-range is visible up to wavelengths well above 100 km. This seemingly large difference could lead us to doubt whether the calculated structure functions do actually correspond to the spectrum given by Nastrom *et al.* (1984). We shall show below that there is, in fact, a very good correspondence.

We note that the agreement with the two-dimensional isotropic relation (53) is better for large separations than for small separations. This can also be seen by comparing the values of the calculated constants in (69) with their expected isotropic values. Using (53) and (68) we find

$$a_2/a_{2_{Iso}} = 0.67, \quad b_2/b_{2_{Iso}} = 0.92, \quad c_2/c_{2_{Iso}} = 0.90. \tag{70}$$

Without any doubt, this result is contrary to what we would have obtained for a field which was truly two-dimensional in the whole measured interval. For such a field the agreement with isotropic relations would have been as least as good for small separations as for large separations. Thus, we must interpret the small separation deviation from the isotropic relation as a sign of three-dimensional effects becoming important for these separations. A comparison with the three-dimensional isotropic relation shows that $a_2/a_{2_{Iso3D}} = 0.83$. There is, of course, no reason to expect that the measured structure functions should agree with three-dimensional isotropic relations. Unfortunately, no direct comparison with the axisymmetric relation (54) can be made, since the vertical velocity component was not measured. However, the deviation from the two-dimensional relation shows us that the last term in (54) is of the same order as the two other terms, indicating that the ratio between the typical vertical and horizontal velocity scales is of the same order as the ratio between the corresponding length scales.

The agreement with the relation (69) is very good for the transverse structure function while the corresponding agreement is only reasonably good for the longitudinal structure function. The deviation of the longitudinal structure function from relation (68) is statistically significant, even though it is rather small. Calculations on subsets of the whole data set gave curves which were practically indistinguishable from the curve in figure 3. We can also note that the deviation of the measured curves from (68) and (69) at separations larger than 2000 km is positive. This means that it cannot be due to a measurement error caused by the use of Taylor's hypothesis, since such an error should lead to an underestimate of the structure function. To test the logarithmic dependence in the large-scale regime we have subtracted the $r^{2/3}$-terms in (68) and (69) from our calculated structure function points, and then divided them by r^2. The result is plotted in a lin-log diagram in figure 4. The agreement with a logarithmic curve is almost perfect from about 60 to 1800 km for the transverse structure function and from about 300 to 1800 km for the longitudinal structure function. This agreement is of course strong evidence supporting the enstrophy inertial range hypothesis.

To test the $r^{2/3}$-dependence of the small-scale data we have subtracted the last two terms in (68) and (69) from the calculated function points and plotted the remaining parts in figure 5 and figure 6. For the transverse structure function there is a very close agreement to an $r^{2/3}$-dependence up to separations of about 400 km and a rather close agreement up to separations larger than 1000 km, while the agreement, again, is less good for the longitudinal structure function. For the transverse structure function the subtracted term is about ten times larger than the remaining term for large separations. Yet, the remaining term follows a $r^{2/3}$-curve pretty closely.

Thus, we have found that the calculated structure functions, with a high degree of accuracy, can be split into two different types of terms according to the relation (66). At small separations they follow a $r^{2/3}$-dependence and at large separations a $r^2 \ln r$-dependence with an extra r^2-term. The two ranges clearly overlap in the region of about 100 km. In the $r^{2/3}$-range the structure functions are far from the two-dimensional isotropic relation, while they are closer to it in the $r^2 \ln r$-range.

Given the values of the constants a_1, c_1, a_2 and c_2 we can calculate the one-

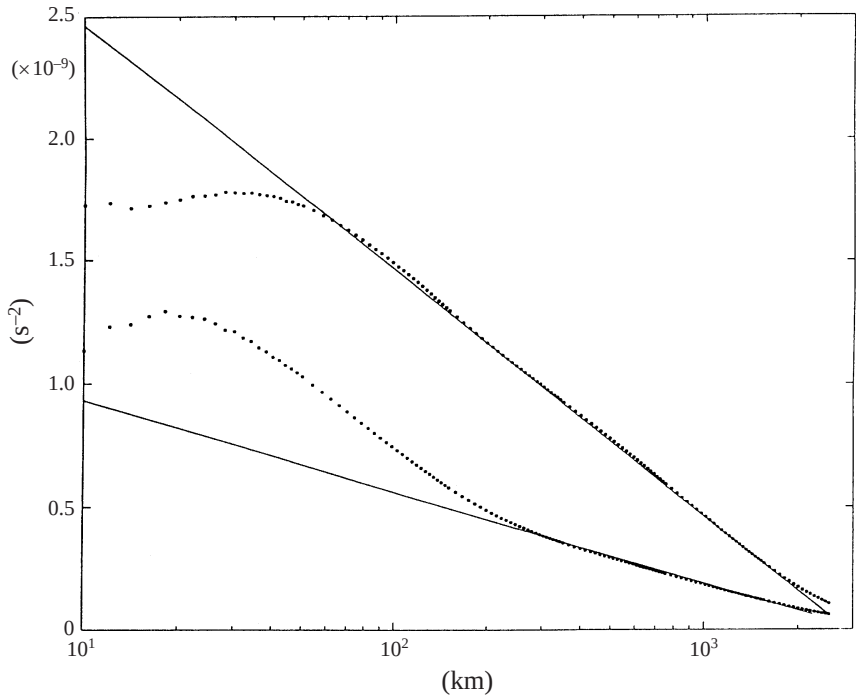

FIGURE 4. Transverse and longitudinal second-order structure functions versus separation distance. Upper curve is the transverse function. The $r^{2/3}$-terms in (68) and (69) have been removed and the remaining points divided by r^2. Solid lines are curves given by the last two terms in (68) and (69) divided by r^2.

dimensional energy spectrum that we would have obtained if the structure functions followed the relations (68) and (69) in an infinitely extended region. According (67) we obtain

$$E_1(k) = d_1 k^{-5/3} + d_2 k^{-3}, \tag{71}$$

where $d_1 \approx 0.12(a_1 + a_2) \approx 9.1 \times 10^{-4}$ and $d_2 = 0.5(c_1 + c_2) \approx 3.0 \times 10^{-10}$ (with units in metres and seconds). In figure 7 we have plotted this spectrum together with the data points given by Nastrom *et al.* (1984). The spectra of Nastrom *et al.* are zonal and meridional power spectra (without the factor 0.5). Half the sum of the two spectra should therefore give the energy spectrum, and since the two spectra are very similar each of them is very close to the energy spectrum. Given the fact that our spectrum is computed on a different data set with a completely different method, we find the agreement remarkably good.

7.2. *Fourth- and third-order structure functions*

We first present the results for the fourth-order structure functions, since we think that these results will explain the poor convergence of the third-order structure function, especially for small separations. In figure 8 we have plotted the longitudinal flatness factor

$$F_L = \frac{\langle \delta u_L \delta u_L \delta u_L \delta u_L \rangle}{\langle \delta u_L \delta u_L \rangle^2} \tag{72}$$

and the corresponding transverse flatness factor. For a Gaussian probability distribution the flatness factor is equal to 3. In figure 8 we can see that the calculated

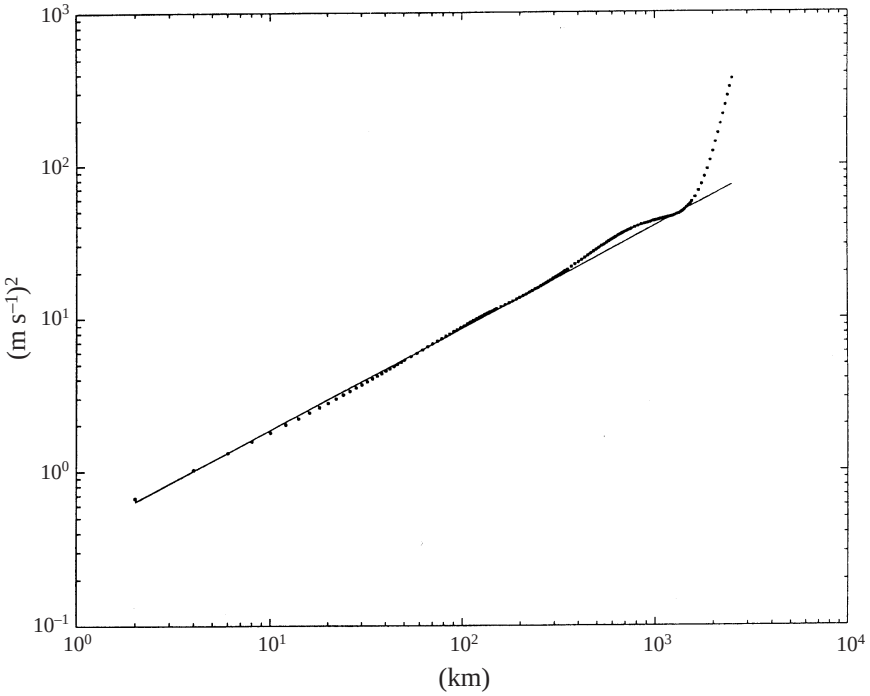

FIGURE 5. Transverse structure function versus separation distance. The last two terms in (69) have been removed. Solid line is the first term in (69).

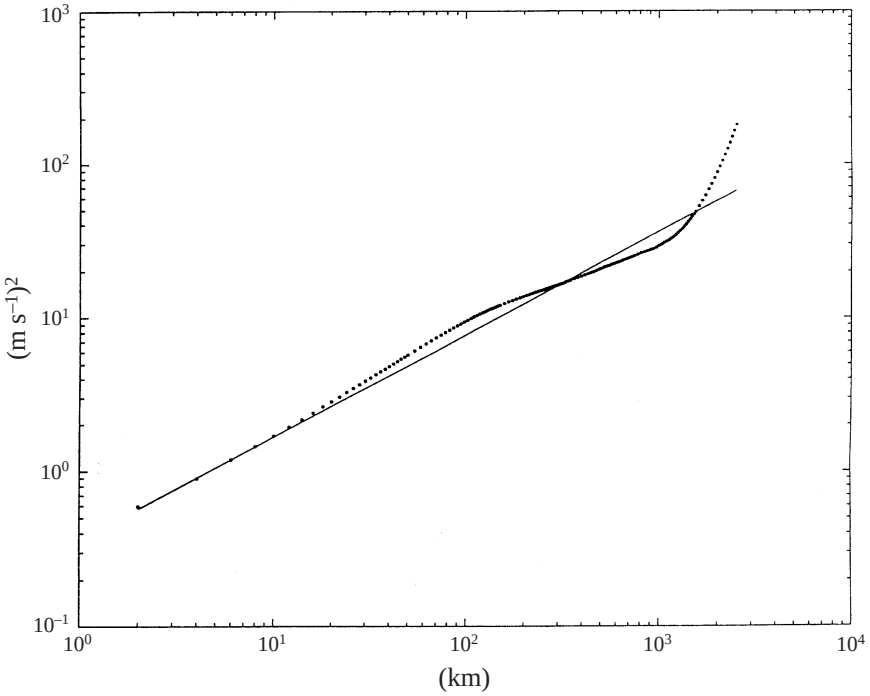

FIGURE 6. Longitudinal structure function versus separation distance. The last two terms in (68) have been removed. Solid line is the first term in (68).

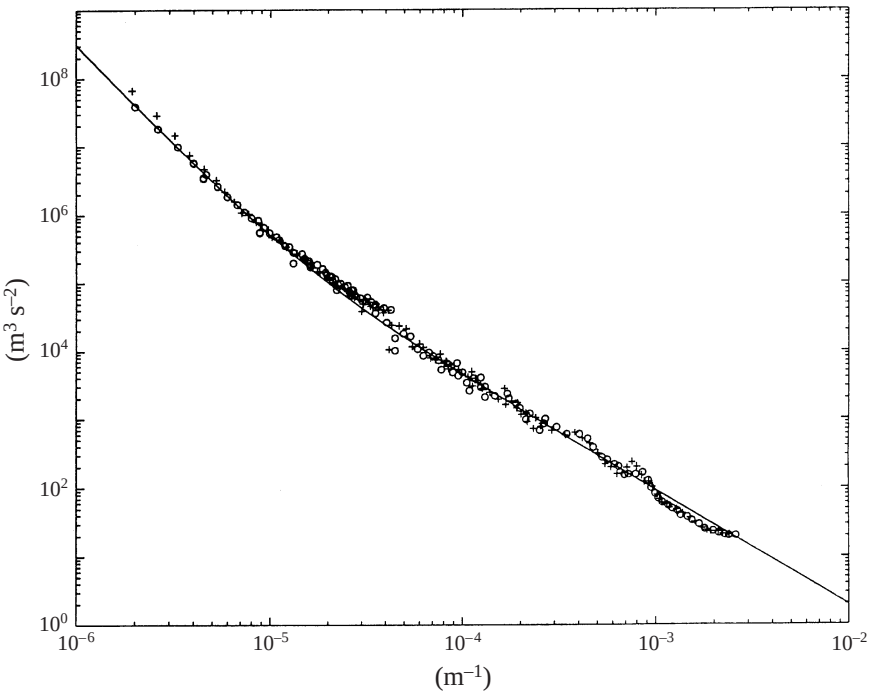

FIGURE 7. Energy spectrum according to (71), together with the data points given by Nastrom *et al.* (1984). Circles: zonal wind power spectrum. Crosses: meridional wind power spectrum.

flatness factors grow very fast at small separations. Again, we want to emphasize that the results are very well converged, and that calculations on subsets of the whole data set gave practically identical results. Frisch (1995) defines intermittency at small scales as equivalent to a flatness factor growing without bound for small scales. Here we have found a case which closely corresponds to this definition of intermittency. According to the Kolmogorov (1941) theory the flatness factor should be constant in the energy inertial range of three-dimensional turbulence, while intermittency theories (see Frisch 1995) predict a weak power law increase of the flatness factor as the separation decreases. Van Atta & Chen (1970) measured a flatness factor following a power law $r^{-0.1}$ in the energy inertial range of an atmospheric boundary layer over the ocean. The highest values measured were of the order of 10. Van Atta & Antonia (1980) have made a survey of different experimental values of the flatness factor of the velocity derivative, which is the single-point limit of (72). The highest flatness factors are found in high Reynolds number atmospheric boundary layers and are around 30. Here we have found a two-point flatness factor which is increasing roughly as $r^{-3/2}$ for small separations and reaching values of two order of magnitudes larger than previously have been measured. We shall not pursue this result further here, but only use it to explain the very slow convergence of the third-order structure functions. That the flatness factor is high means that the tails of the probability distribution are wide. The tails correspond to relatively rare but high-amplitude events. There will be two contributions to the third-order structure function from such events, one large positive and one large negative contribution. The result comes out as a difference between these two contributions and is itself very small compared to each of them. Therefore, the convergence is very slow.

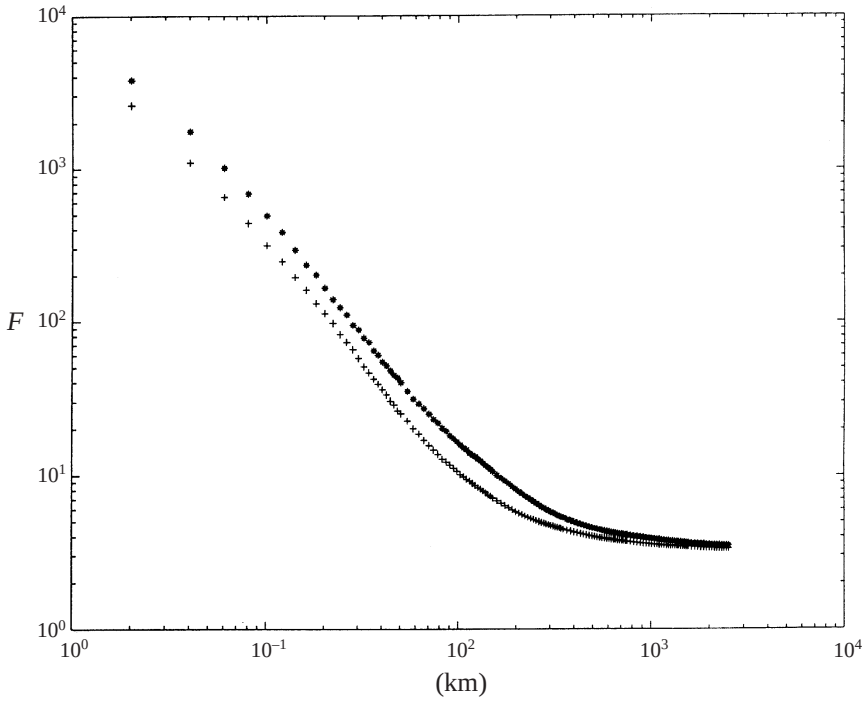

FIGURE 8. Longitudinal (crosses) and transverse (stars) flatness factors versus separation distance.

In figure 9 we have plotted the third-order structure functions $\langle \delta u_L \delta u_L \delta u_L \rangle$, $\langle \delta u_L \delta u_T \delta u_T \rangle$ together with their sum in the interval [20, 1000] km. There is considerable scatter for separations up to 30 km. The curves are reasonably converged in the interval [30, 300] km. Calculations on subsets of the data gave similar results in this interval. First, we note that the third-order structure functions are positive in the measured interval, in contrast to previously reported measurements of these functions elsewhere in nature (e.g. Van Atta & Chen 1970; Van Atta & Park 1980; Antonia *et al.* 1995). This must be explained by the fact that two-dimensional effects are important in our case, whereas three-dimensional effects have been dominant in the previously reported cases.

Next, we note that there is a narrow range between 30 and 70 km where the curves follow a r^3-dependence. It is also possible that this dependence would continue for smaller separations if those could be measured more accurately. The two functions are also quite close to each other in this region, not too far from the isotropic relation which says that they should be identical. Despite the fact that the measured r^3-range is narrow we interpret it as a sign of a positive two-dimensional enstrophy flux, in accordance with (22) or (34). These relations are asymptotic relations for r which are both much larger than a typical viscous length scale and much smaller than a typical large length scale in which enstrophy is generated. It can hardly be doubted that we are far from both a typical viscous length and a large length scale. A positive or negative energy flux in this region would contribute with a linear term, but this term would be much smaller than the measured curve, unless the energy flux is unrealistically large. In figure 9 we have also plotted the linear term (dashed line) which we would have obtained with a negative two-dimensional energy flux and a two-dimensional

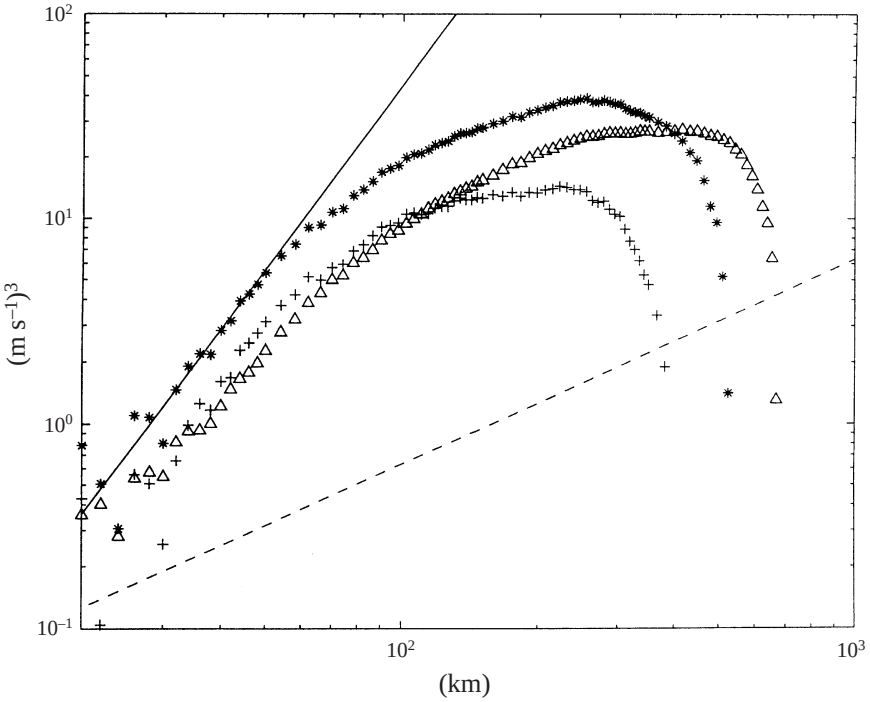

FIGURE 9. Third-order structure functions versus separation distance. Triangles: $\langle \delta u_L \delta u_T \delta u_T \rangle$. Crosses: $\langle \delta u_L \delta u_T \delta u_T \rangle$. Stars: the sum of the two functions. Solid line: ar^3 with $a = 4.5 \times 10^{-10} \mathrm{s}^{-3}$. Dashed line: linear term corresponding to an estimated two-dimensional energy flux.

Kolmogorov constant of $C_0 = 6$, given our second-order structure function data. This term is much smaller than the measured curve. To calculate the term we have used the trace of our measured second-order structure function and the relation (52). This gave us the estimated two-dimensional energy flux $|\Pi_u| \approx 3.0 \times 10^{-6}\,\mathrm{m^2\,s^{-3}}$. In a 10 km layer with a density of $0.5\,\mathrm{kg\,m^{-3}}$ this would correspond to a flux of $0.015\,\mathrm{W\,m^{-2}}$ which is very small by any comparison. Even if we only were interested in its sign, we would still have to measure the third-order structure function accurately for separations of the order of some few kilometres, in order to determine such a small energy flux, and this would require an enormous amount of data. Another problem is that the assumption of two-dimensionality is hardly justified for these small scales. To explain the deviation from the two-dimensional isotropic relation which the second-order curves exhibit, we must take the vertical velocity component into account. If this component is dynamically important there is a three-dimensional energy flux which must be computed by also taking this component into account.

Interpreting the data as evidence of an enstrophy inertial range we can measure the average enstrophy flux in the atmosphere as

$$\Pi_\omega = (1.8 \pm 0.3) \times 10^{-13}\,\mathrm{s^{-3}}, \tag{73}$$

where we have used the relations (22) or (34) and (47) and the measured sum of the two functions. This is much larger than a previous estimate $\Pi_\omega \sim 10^{-15}\mathrm{s}^{-3}$, by Charney (1971). The error estimate is based on results calculated from the four subsets of the data. Given the second-order data the constant $\mathscr{K}$ can be calculated as

$$\mathscr{K} = 0.19 \pm 0.03. \tag{74}$$

Although this value is reasonably close to unity, it is lower than expected. Maltrud & Vallis (1991) obtained values of $\mathscr{K}$ varying around unity with mean value 0.7, in low Reynolds number DNS of forced β-plane turbulence. Leith & Kraichnan (1972) calculated $\mathscr{K}$ as 1.74, using the test field model.

The average kinematic viscosity at an altitude of 10 000 m can be estimated as $\nu = 3.4 \times 10^{-5}\,\mathrm{m^2\,s^{-1}}$. This gives the enstrophy dissipation length scale $\eta_\omega = \nu^{1/2}/\Pi_\omega^{1/6} \approx 0.6\,\mathrm{m}$. This is the viscous length scale of vertical vorticity which we would be able to measure if the atmosphere could be treated as a two-dimensional system down to scales of this size. This is, of course, not the case. This length scale is probably of no relevance, since three-dimensional effects and vortex stretching must become important for larger scales than this. We shall refrain from giving any estimate of the relevant smallest length scale. Instead we shall give the velocity and vorticity structure functions in the logarithmic region, when our data have been scaled with a large length scale L, which we choose as the radius of the Earth. If the $r^{2/3}$-term is removed these expressions become

$$\langle \delta\omega\delta\omega \rangle = 4\Omega + \left(4\mathscr{K} \ln\left(\frac{r}{L}\right) + 4G\right)\Pi_\omega^{2/3}, \tag{75}$$

$$\langle \delta\boldsymbol{u}\cdot\delta\boldsymbol{u} \rangle = \left(\mathscr{K} - G - \mathscr{K}\ln\left(\frac{r}{L}\right)\right) r^2\Pi_\omega^{2/3}, \tag{76}$$

where $G \approx 0.37$. We find it satisfying that we also obtain a value of order of unity for the constant G.

8. Summary and conclusions

We have found that the measured second-order structure functions can be divided into two different types of terms, one of which gives the $k^{-5/3}$-range and the other the k^{-3}-range. The measured second-order structure functions are very well converged and very smooth, compared to previously reported spectral measurements. The logarithmic term, giving the k^{-3}-spectrum, is more clearly displayed in real space than the corresponding term in Fourier space. For the $r^{2/3}$-term the situation is reversed. The $k^{-5/3}$-range in Fourier space is much more apparent than the corresponding range in real space, if no separation of terms is made in the structure function data. However, there is a very good correspondence between the two descriptions, as our comparison with the data of Nastrom *et al.* (1984) shows.

The calculated structure functions and the corresponding spectrum show that one should be very careful when one compares scaling ranges of different methods. A scaling range which is very apparent in one formulation could be hard to detect in another formulation. Bacmeister *et al.* (1996) have computed wavelet power spectra of airplane wind data taken at high altitude. In the region 1–100 km, they found no single power law dependence of the wavelet spectra and the slope varied between $-5/3$ and -3. They found these results incompatible with the single $k^{-5/3}$-dependence for the Fourier power spectrum observed in previous measurements in the same wavenumber region, for example by Nastrom *et al.* (1984). We find it likely that the $k^{-5/3}$ Fourier spectrum was inherent even in the data used by Bacmeister *et al.*, and that they would have observed it if they had calculated the Fourier spectrum. In a certain wavelength interval there is no simple one-to-one correspondence between the slopes of two power spectra calculated using two completely different sets of base functions. Therefore, one should not be very surprised that the wavelet spectrum did not have the same simple form as the Fourier spectrum.

The second-order structure functions agree better with the two-dimensional isotropic relation for larger separations than for smaller separations. This suggests that the $k^{-5/3}$-range cannot satisfactorily be explained as a two-dimensional inertial range spectrum, but that the k^{-3}-range could be explained as a two-dimensional enstrophy inertial range spectrum. The structure function measurements have made it more clear that the k^{-3} spectrum range, alternatively the logarithmic structure function range, does indeed exist in the atmosphere. Moreover, this range is wider than previous measurements have indicated. For the transverse structure function the logarithmic region is visible down to separations of about 60 km. Smith & Yakhot (1994) have suggested that effects of the finite size of the Earth can explain the existence of the k^{-3}-range. We find it difficult to believe that such effects could be visible at such small scales as 60 km. It is more reasonable to interpret this range as an enstrophy inertial range in the classical sense.

The very clean logarithmic curve (figure 4) of the transverse structure function shows that the energy spectrum must be a correspondingly clean k^{-3}-curve in the enstrophy inertial range. In numerical simulations of two-dimensional turbulence a steeper spectrum, $k^{-3-\alpha}, 0 < \alpha < 1$, is usually observed. It is often argued that this is due to the presence of singularities or coherent structures. For example, Gilbert (1988) found a spectrum of the form $k^{-11/3}$, using a model consisting of spiralling coherent vortices. Since a lin-log plot is far more sensitive than a log-log plot we can be pretty sure that the slope of the energy spectrum must be -3.0, rather than anything else. An $\alpha \neq 0$ would give a power law r^{α}, rather than a logarithmic law, for the vorticity structure function and a power law $-r^{2+\alpha}$ for the velocity structure function. Any $\alpha > 0.05$ would have given us a curve clearly different from that we can see in figure 4. However, the logarithmic range is not sufficiently wide for any safe conclusion as to whether the energy spectrum has the pure form k^{-3} as suggested by Kraichnan (1967) and Batchelor (1969), or the form $k^{-3}(\ln(k/k_1))^{-1/3}$, as suggested by Kraichnan (1970). We have performed some numerical investigations to test how wide an energy spectrum range of the form $k^{-3}(\ln(k/k_1))^{-1/3}$ must be for the corresponding vorticity structure function to show any visible deviation from a logarithmic dependence. The conclusion is that the spectrum range, as well as the corresponding structure function range, must be several decades wide for such a deviation to become visible.

We found a dramatic increase in the flatness factor of the longitudinal and the transverse velocity components for smaller scales, of the order of some kilometres. For the smallest scales we found flatness factors well above 1000. We note that this is very far from flatness factors between 3 and 8 found by Smith & Yakhot (1995) in DNS of a two-dimensional energy inertial range. In an experimental study of thin layers of an electrolyte Paret & Tabeling (1998) found that the two-dimensional inverse energy cascade is non-intermittent and that the flatness factor is constant in such a range. If the high and increasing flatness factors are associated with the $k^{-5/3}$-range, then we cannot interpret this range as a two-dimensional energy inertial range, nor as a three-dimensional Kolmogorov inertial range. However, the high and increasing flatness factors might be associated with the enstrophy cascade and the k^{-3}-spectrum, rather than the $k^{-5/3}$-spectrum, although they are visible at separations of the order of some kilometres. The enstrophy cascade may very well continue down to such small scales, although it is not apparent when we study the second-order structure functions. The results for the third-order structure functions indicate that the enstrophy cascade does indeed continue down to rather small scales, and if this cascade is very intermittent, it could very well be that the high flatness factors are associated with this process, rather than with anything else.

The very high flatness factors explain the slow convergence of the third-order structure functions, which could be satisfactorily evaluated only in the interval [30, 300] km. In this interval the third-order structure functions were positive, indicating that two-dimensional effects are important here. We also found a short interval [30, 70] km where the third-order structure functions followed a r^3-dependence. Although this range is rather narrow we suggest that it can be interpreted as a sign of a two-dimensional enstrophy flux in accordance with the relation (22). Using this relation we could calculate the average enstrophy flux and determine the constant $\mathscr{K}$. To our knowledge, this is the first reported measurement of these quantities. The fact that we do not observe a linear dependence for these rather small separations is not very surprising, since a linear term, due to a positive or negative energy flux, would be much smaller than the measured curve. However, the fact that the cubic dependence does not continue for larger separations than 70 km, is a little surprising, and could be a remaining source of doubt as to whether the k^{-3} spectrum and the corresponding logarithmic structure function can indeed be explained as evidence of a two-dimensional enstrophy inertial range. However, since the third-order structure function is indeed positive and cubic, although in a very limited range, and since we have measured a very clean logarithmic second-order structure function, we find it difficult not to interpret the results as evidence of a positive enstrophy flux.

As for the energy flux, on the other hand, it could not be measured, for two reasons. First, the third-order structure functions could not be measured for the small separations where we could expect to find a linear term. Secondly, even if a linear term could be measured, the energy flux could not have been determined with any certainty, since the assumption of two-dimensionality is not justified for such small separations, as the result for the seond-order structure functions clearly shows.

Our results can be interpreted as evidence of two fields, originating from two different sources and only weakly interacting: a two-dimensional vorticity field which is dominant at larger scales, and a three-dimensional field which is dominant at smaller scales. The deviation of the longitudinal structure function from the simple split of terms in the region of about 100 km could be interpreted as evidence of a weak interaction between the two fields. To what extent the two fields really do coexist in space and time is an interesting problem which could be the objective of a future investigation. What physical mechanism there could be behind the three-dimensional field is an open question. The transverse structure function result (figure 5) indicates that this field coexists with the two-dimensional vorticity field up to scales of about 1000 km. Long gravity waves breaking down to shorter waves, as suggested by Dewan (1979), could be a reasonable explanation. Another interesting possibility suggested by Professor J. C. R. Hunt (private communication) is that the $k^{-5/3}$-spectrum might be associated with small to large-scale micro to macro fronts that can be found in stratified flows, especially with rotation. This suggestion deserves further investigation.

To conclude, we would very much like to give the answer to the question asked in the title: Can the atmospheric kinetic energy spectrum be explained by two-dimensional turbulence? As all answers in natural science it will, of course, contain a certain amount of uncertainty. The lower-wavenumber part of the spectrum, exhibiting a k^{-3}-range, can be interpreted as a two-dimensional enstrophy inertial range. The higher-wavenumber part of the spectrum, exhibiting a $k^{-5/3}$-range cannot be explained by the two-dimensional turbulence theory.

I thank the MOZAIC program and Dr Alain Marenco for providing me with the MOZAIC data. I also thank the following persons who have made different con-

tributions to this work: Professors Greg Nastrom, Arne Johansson, Uriel Frisch & Hilding Sundquist, Drs Arne Nordmark, Tony Burden & Erik Aurell. Financial support from the Swedish Research Council for Engineering Sciences (TFR) is gratefully acknowledged.

Appendix. Isotropic relations for two-dimensional structure functions

In this Appendix we derive the isotropic relations (53) and (23) for the second- and third-order two-dimensional structure functions.

The second-order structure tensor function can be written

$$\langle \delta u_i \delta u_j \rangle = n_i n_j \langle \delta u_L \delta u_L \rangle + s_{ij} \langle \delta u_T \delta u_T \rangle, \tag{A 1}$$

where $s_{ij} = \delta_{ij} - n_i n_j$, and $\boldsymbol{n} = \boldsymbol{r}/r$ is the unit vector in the direction of $\boldsymbol{r}$. By the condition of incompressibility we have

$$\frac{\partial}{\partial r_i} \langle \delta u_i \delta u_j \rangle = 0. \tag{A 2}$$

Applying this condition to (A 1) and using the relations

$$\frac{\partial}{\partial r_i} n_j = \frac{1}{r} s_{ij}, \tag{A 3}$$

$$\frac{\partial}{\partial r_l} s_{ij} = -\frac{1}{r}(n_i s_{lj} + n_j s_{li}), \tag{A 4}$$

we immediately arrive at (53).

To derive (23) we first define the tensor

$$D_{ijk} = \langle u_i u_j u_k' \rangle. \tag{A 5}$$

By incompressibility we have

$$\frac{\partial}{\partial r_k} D_{ijk} = 0. \tag{A 6}$$

In the isotropic case we can write

$$D_{ijk} = n_i n_j n_k a(r) + s_{ij} n_k b(r) + (s_{ik} n_j + s_{jk} n_i) c(r), \tag{A 7}$$

where a, b and c are scalar functions which by incompressibility are found to be related through

$$b = -a, \quad c = \frac{1}{2} \frac{\mathrm{d}}{\mathrm{d}r}(ra). \tag{A 8}$$

The third-order structure tensor function can be written as

$$\langle \delta u_i \delta u_j \delta u_k \rangle = 2D_{ijk} + 2D_{jki} + 2D_{kij}, \tag{A 9}$$

from which we find

$$\langle \delta u_L \delta u_L \delta u_L \rangle = 6a, \quad \langle \delta u_L \delta u_T \delta u_T \rangle = 2b + 4c. \tag{A 10}$$

By combining these relations with the relations derived from incompressibility we arrive at (23)

REFERENCES

Antonia, R. A., Ould-Rouis, M., Anselmet, F. & Zhu, Y. 1997 Analogy between predictions of Kolmogorov and Yaglom. *J. Fluid Mech.* **332**, 395–409.

Antonia, R. A., Zhu, Y. & Hosokawa, I. 1995 Refined similarity hypotheses for turbulent velocity and temperature fields. *Phys. Fluids* **7**, 1637–1648.

Bacmesiter, J. T., Eckermann, S. D., Newman, P. A., Lait, L., Chan, K. R., Loewenstein, M., Proffitt, M. H. & Gary, B. L. 1996 Stratospheric horizontal wavenumber spectra of winds, potential temperature, and atmospheric tracers observed by high-altitude aircraft. *J. Geophys. Res.* **101**, 9441–9470.

Balsley, B. B. & Carter, D. A. 1982 The spectrum of atmospheric velocity fluctuations at 8 km and 86 km. *Geophys. Res. Lett.* **9**, 465–468.

Batchelor, G. K. 1953 *Homogeneous Turbulence*. Cambridge University Press.

Batchelor, G. K. 1969 Computation of the energy spectrum in homogeneous two-dimensional decaying turbulence. *Phys. Fluids* **12**, suppl. II233–II239.

Charney, J. G. 1971 Geostrophic turbulence. *J. Atmos. Sci.* **28**, 1087–1095.

Dewan , E. M. 1979 Stratospheric spectra resembling turbulence. *Science* **204**, 832–835.

Frisch, U. 1995 *Turbulence*. Cambridge University Press.

Gage, K. S. 1979 Evidence for a $k^{-5/3}$ law inertial range in mesoscale two-dimensional turbulence. *J. Atmos. Sci.* **36**, 1950–1954.

Gage, K. S. & Nastrom, G. D. 1986 Theoretical interpretation of atmospheric spectra of wind and temperature observed by commercial aircraft during gasp. *J. Atmos. Sci.* **43**, 729–740.

Gilbert, A. 1988 Spiral structures and spectra in two-dimensional turbulence. *J. Fluid Mech.* **193**, 475–497.

Kao, S. K. & Wendell L. L. 1970 The kinetic energy of the large-scale atmospheric motion in wavenumber-frequency space. *J. Atmos. Sci.* **27**, 359–375.

Kolmogorov, A. N. 1941*a* The local structure of turbulence in incompressible viscous fluid for very large Reynolds number. *Dokl. Akad. Nauk SSSR* **30**(4). English translation in *Proc. R. Soc. Lond.* A **434** (1991), 9–13.

Kolmogorov, A. N. 1941*b* Dissipation of energy in the locally isotropic turbulence'. *Dokl. Akad. Nauk SSSR* **32**(1). English translation in *Proc. R. Soc. Lond.* A **434** (1991), 15–17.

Kraichnan, R. H. 1967 Inertial ranges in two-dimensional turbulence. *Phys. Fluids* **10**, 1417–1423.

Kraichnan, R. H. 1970 Inertial-range transfer in two- and three-dimensional turbulence. *J. Fluid Mech.* **47**, 525–535.

Leith, C. E. & Kraichnan, R. H. 1972 Predictability of turublent flows. *J. Atmos. Sci.* **29**, 1041.

Lighthill, M. J. 1959 *Introduction to Fourier Analysis and Generalised Functions.* Cambridge University Press.

Lilly, D. K. 1989 Two-dimensional turbulence generated by energy sources at two scales. *J. Atmos. Sci.* **46**, 2026–2030.

Lindborg, E. 1995 Kinematics of homogeneous axisymmetric turbulence. *J. Fluid Mech.* **302**, 179–201.

Lindborg, E. 1996 A note on Kolmogorov's third-order structure-function law, the local isotropy hypothesis and the pressure-velocity correlation. *J. Fluid Mech.* **326**, 343–356.

Maltrud, M. E. & Vallis, G. K. 1991 Energy spectra and coherent structures in forced two-dimensional and beta-plane turbulence. *J. Fluid Mech.* **228**, 321–342.

Marenco, A., Thouret V., Nédélec, P., Smith, H., Helten M., Kley, D., Karcher, F., Simon, P., Law, K., Pyle, J., Poschmann, G., Von Wrede, R., Hume, C. & Cook, T. 1998 Measurement of ozone and water vapor by airbus in-service aircraft: the MOZAIC airborne program, an overview. *J. Geophys. Res. Atmos.* **103**, 25631–25642.

Millikan, C. B. 1939 A critical discussion of turbulent flows in channels an circular tubes. *Proc. Fifth Intl Congr. Applied Mechanics*, pp. 386–392. Cambridge, MA.

Nastrom, G. D. & Gage, K. S. 1985 A climatology of atmospheric wavenumber spectra of wind and temperature observed by commercial aircraft. *J. Atmos. Sci.* **42**, 950–960.

Nastrom, G. D., Gage, K. S. & Jasperson, W. H. 1984 Kinetic energy spectrum of large- and mesoscale atmospheric processes. *Nature* **310**, 36–38.

Paret, J. & Tabeling, P. 1998 Inverse energy cascade in 2D turbulence: experimental study. *Advances in Turbulence VII*. Kluwer.

Saddoughi, S. G. & Veeravalli, S. V. 1994 Local isotropy in turbulent boundary layers at high Reynolds number. *J. Fluid Mech.* **268**, 333–372.

Smith, L. M., Chasnov, J. R. & Waleffe, F. 1996 Crossover from two- to three-dimensional turbulence. *Phys. Rev. Lett*. **77**, 2467–2470.

Smith. L. M. & Yakhot. V. 1994 Finite-size effects in forced two-dimensional turbulence. *J. Fluid Mech.* **274**, 115–138.

Van Atta, C. W. & Chen, W. Y. 1970 Structure functions of turbulence in the atmospheric boundary layer over the ocean. *J. Fluid Mech.* **44**, 145–159.

Van Atta, C. W. & Park, J. T. 1980 Hot- and cold-wire sensitivity corrections for moments of the fine scale turbulence in heated flows. *Phys. Fluids* **23**, 701–705.

Van Atta, C. W. & Antonia, R. A. 1980 Reynolds number dependence of skewness and flatness factors of turbulent velocity derivatives. *Phys. Fluids* **23**, 252–257.

VanZandt, T. E. 1982 A universal spectrum of buoyancy waves in the atmosphere. *Geophys. Res. Lett*. **9**, 575–578.

Vinnichenko, N. K. 1970 The kinetic energy spectrum in the free atmosphere — 1 second to 5 years. *Tellus* **22**, 158–166.